ETV7 represses a subset of interferon-stimulated genes that restrict influenza viruses

Heather M. Froggatt[1], Alfred T. Harding[1], and Nicholas S. Heaton[1,*]

[1]Department of Molecular Genetics and Microbiology
Duke University School of Medicine
Durham, NC 27710

Keywords:

CRISPRa, screening, type I interferon, interferon-stimulated genes, gene regulation

*To whom correspondence should be addressed:
Nicholas S. Heaton, PhD
Assistant Professor
Department of Molecular Genetics and Microbiology (MGM)
Duke University Medical Center
213 Research Drive, 426 CARL Building, Box 3054
Durham, NC 27710
Tel: 919-684-1351
Fax: 919-684-2790
Email: nicholas.heaton@duke.edu

Abstract

The type I interferon (IFN) response is an important component of the innate immune response to viral infection. Precise control of interferon responses is critical, as insufficient levels of interferon-stimulated genes (ISGs) can lead to a failure to restrict viral spread, while excessive ISG activation results in interferon-related pathologies. While both positive and negative regulatory factors can control the magnitude and duration of IFN signaling, it is also appreciated that a number of ISGs regulate aspects of the interferon response themselves. However, the mechanisms underlying complex ISG regulatory networks remain incompletely defined. In this study, we performed a CRISPR activation screen to identify new regulators of type I IFN responses. We identified ETS variant transcription factor 7 (ETV7), a strongly induced ISG, as a protein that acts as a negative regulator of the type I IFN response; however, ETV7 did not uniformly suppress ISG transcription. Instead, ETV7 specifically targeted a subset of ISGs for regulation based on their promoter sequences. We further showed the subset of ETV7-modulated ISGs is particularly important for control of influenza viruses. Together, our data demonstrate that ETV7 is a component of the complex ISG regulatory network by controlling the expression of a subset of ISGs with a potential role in directing the interferon response against specific viruses.

60 **Significance**

61 Interferons (IFNs) were first described in 1957 and are now known to be critical for
62 restriction of viruses. Still, our understanding of the complex web of interactions that
63 underlie IFN responses remains incomplete. In particular, negative regulation of interferon
64 responses has received disproportionately less study. In this work, we performed a
65 genome-wide overexpression screen for factors capable of suppressing IFN response
66 signaling. We identified a DNA binding transcription factor (ETV7) that, after induction by
67 interferon, acts to suppress a subset of IFN-stimulated genes required for control of
68 influenza viruses. Our work highlights the importance of understanding negative IFN
69 signaling not only with respect to the magnitude and duration of the response, but also
70 the specificity of its antiviral effects.

Introduction

The type I interferon (IFN) response is a transient innate immune defense system that, upon activation by viral infection, induces the transcription of hundreds of interferon-stimulated genes (ISGs) (1). Many ISGs have characterized antiviral roles that restrict viral replication by either interfering with viral processes directly or regulating the cellular pathways required for viral replication (2). However, because replication mechanisms and points of interaction with the cell differ between viruses, individual ISGs have varying potencies against different viruses (3–5). As a result, unique combinations of ISGs are thought to mediate successful antiviral responses against distinct viruses (1, 6).

The activation of the type I IFN signaling pathway in response to viral infection is well understood (7, 8). Extracellular IFN, which is released after a cell recognizes virus-derived nucleic acid, is bound by its cognate plasma membrane-localized receptor (IFNARs). Downstream effectors (JAK proteins) are phosphorylated to then activate interferon-stimulated gene factor 3 (ISGF3) complex formation. Finally, the ISGF3 complex of STAT1, STAT2, and IRF9 translocates to the nucleus (7). There, ISGF3 binds the interferon sensitive response element (ISRE), with the consensus DNA motif GAAANNGAAA, to activate transcription of ISGs (9).

As infection is cleared and virally derived innate immune activators become scarce, interferon production is reduced and the interferon-stimulated gene response is downregulated. To facilitate this return to cell homeostasis, negative regulators are induced and act at multiple levels in the signaling pathway (10). For example, PKD2 is an

ISG that recruits ubiquitin to the IFN receptor, IFNAR1, resulting in its degradation (11). SOCS1 and SOCS3 are upregulated during, and act to limit, the IFN response through direct interactions with JAK proteins, while SOCS1 also ubiquitinates other pathway components (12). USP18 is induced by IFN to help return the cell to homeostasis by removing the ubiquitin-like ISG15 from target proteins (13). Thus, negative regulators of IFN responses are an important group of IFN-stimulated genes that control the duration of ISG induction and activity.

In addition to activating or suppressing IFN responses, there are a number of interferon-induced regulators that enhance, limit, or fine-tune antiviral activity (14). Many ISGs themselves participate in innate immune signaling to amplify IFN, and other pro-immune, responses. For example, IFN signaling increases the levels of STAT1/2 and IRF9, thus forming a positive feedback loop that enhances further ISG expression (15). Activators also add complexity by inducing non-canonical IFN response pathways or specific groups of ISGs. Interferon responsive factors (IRFs) 1 and 7 are ISGs and transcription factors that activate subsets of ISGs (16, 17). Recent work has shown ELF1 (E74-like ETS transcription factor) is induced by IFN, resulting in the expression of a group of genes not otherwise activated by the IFN response (18). These differential ISG profiles are thought to allow the cell to fine-tune its antiviral activity for an effective and appropriate response. While interferon-induced positive regulators of the IFN response are known to shape the complexity of ISG activation, reports of analogous roles for negative regulators remain conspicuously absent.

117 To address this gap in knowledge and identify genes able to shape the IFN response
118 through negative regulation, we performed a CRISPR activation (CRISPRa) screen that
119 selected for factors sufficient to prevent expression of an ISRE-containing IFN response
120 reporter. We identified ETV7 (ETS variant transcription factor 7) as a negative regulator
121 of the type I IFN response with a role in controlling the expression of a subset of ISGs.
122 We further showed the ETV7-modulated ISGs are important for control of influenza
123 viruses. Together, these data demonstrate ETV7 is a suppressive component of the
124 complex ISG regulatory network that could be targeted to enhance specific antiviral
125 responses against influenza viruses (1, 19).
126

127 **Results**

128 <u>A CRISPR activation screen identifies potential negative regulators of the type I IFN</u>
129 <u>response.</u>

130 In order to identify negative regulators of the type I IFN response, we developed a type I
131 IFN response reporter (IFNrsp) that included seven copies of the consensus interferon
132 sensitive response element (ISRE) ahead of a minimal CMV promoter controlling
133 expression of sfGFP (**Fig. 1A**). To make our reporter temporally specific, sfGFP was
134 fused to a mouse ornithine decarboxylase (MODC) protein degradation domain to
135 decrease its half-life (20). We stably introduced this construct into the A549 lung epithelial
136 cell line along with a dCAS9-VP64 fusion protein and a MS2-p65-HSF1 activator complex
137 required for the SAM CRISPR activation system (21). After clonal selection, 99.8% of the
138 A549-SAM-IFNrsp cells expressed GFP in response to type I IFN treatment (**Fig. 1B and**
139 **C**). To perform the screen, we took the A549-SAM-IFNrsp cell line and transduced 2×10^8

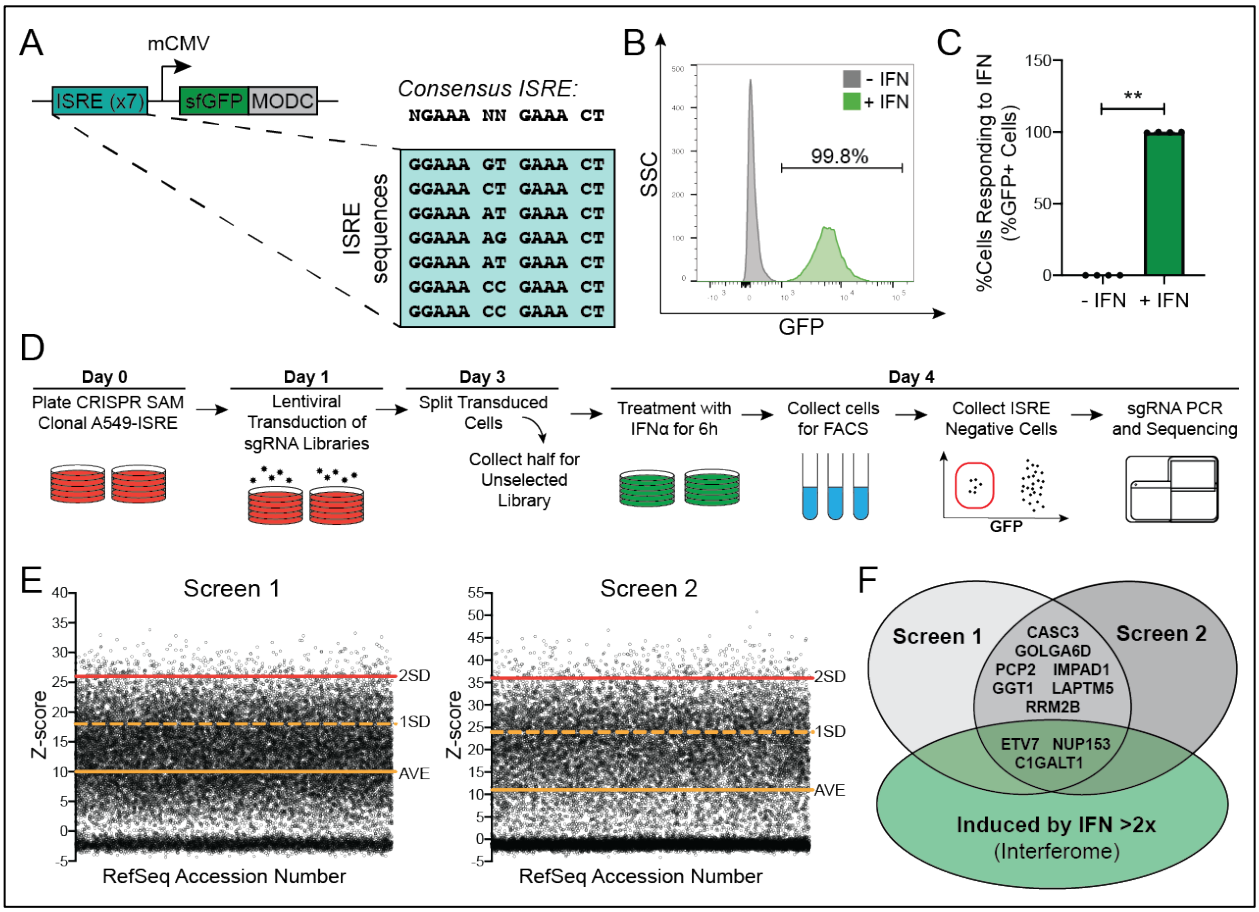

Fig. 1. A CRISPR activation screen to identify negative regulators of the type I interferon response. A) Diagram of the IFN response reporter (IFNrsp) used to identify cells responding to IFN. ISRE = interferon sensitive response element, MODC = protein degradation domain. B) Flow cytometry histogram and C) bar graph of A549-SAM-IFNrsp cells before and after IFN-α treatment (1000 U/mL, 6 h) (data shown as mean ± SD, n=4). Data shown are representative of two independent experiments. P-values calculated using unpaired, two-tailed Student's t-tests, *p<0.05, **p<0.001. D) Diagram of CRISPRa screen workflow to identify negative regulators of the type I IFN response. E) Results of the two independent CRISPRa screens. Z-score values from the replicate screens with a cutoff of 2 standard deviations from the mean were used to identify top "hits". F) Venn diagram indicating overlapping hits from the replicate screens and genes upregulated by interferon at least two-fold, according to the Interferome database (23).

140 cells at a multiplicity of infection (MOI) of 0.5 with a lentivirus library containing sgRNAs

141 designed to activate every putative ORF in the human genome (21) (**Fig. 1D**). After 48

142 hours, half of the cells were collected to determine the transduction efficiency and the

143 remaining cells were re-plated for IFN stimulation. At 72 hours post-sgRNA introduction,

144 the cells were treated with 4,000 U/mL IFN-α for 6 hours and collected for fluorescence-
145 activated cell sorting. During sorting, we eliminated reporter-positive cells and collected
146 only cells that were nonresponsive to IFN, because this population should theoretically
147 be overexpressing a negative regulator of the IFN response. We performed two
148 independent biological replicates of the screen and sequenced the sgRNA-containing
149 amplicons derived from our input DNA, unselected transduced cells, and cells that were
150 nonresponsive to type I IFN. Raw sequencing data was aligned and mapped and
151 subsequently analyzed using the MAGeCK pipeline (22) to generate z-score values for
152 each gene. Genes were defined as "hits" if their z-scores exceeded two standard
153 deviations from the mean, resulting in an overlap of 10 genes between the two screen
154 replicates (**Fig. 1E, Supplementary Data 1 and 2, and Supplementary Table 1**). We
155 were seeking to identify regulators of the IFN response that are regulated by IFN
156 themselves; therefore, we selected hits for validation previously reported to have at least
157 a two-fold induction after IFN stimulation in the Interferome database (23). This analysis
158 identified three hits (C1GALT1, ETV7, and NUP153) as potential negative regulators of
159 the type I IFN response (**Fig. 1F and Supplementary Table 1**).
160
161 <u>Overexpression of ETV7 is sufficient to negatively regulate the type I IFN response.</u>
162 To validate our three hits, and to avoid potential false positive results as the result of off-
163 target effects of CRISPRa, we cloned the three ORFs and validated overexpression of
164 the genes in 293T cells (**Supplementary Figure 1**). Co-transfection of the
165 overexpression plasmids and IFNrsp plasmid, followed by stimulation with IFN-α, resulted
166 in significantly fewer GFP-expressing cells compared to a control mCherry-expressing

167 plasmid (**Fig. 2A and B**). To verify this repressive activity was specific to the IFN response
168 and the hits were not general inhibitors of transcription or translation, we transfected the
169 overexpression plasmids along with a constitutively active GFP-expressing plasmid (**Fig.**
170 **2C**). We included a positive control (EIF2AK1/HRI), which is known to shut off translation
171 when overexpressed (24). C1GALT1 overexpression significantly downregulated GFP
172 expression, indicating the repressive activity of C1GALT1 is not completely specific to the
173 IFN response. While the overexpression of either ETV7 or NUP153 specifically affected
174 the IFNrsp plasmid, NUP153 has previously been shown to control the distribution of
175 STAT1 in the cell (25). We therefore chose ETV7 for further characterization because: 1)
176 ETV7 had not been previously reported to play a role in the IFN response, and 2) it had
177 the strongest inhibitory phenotype against the IFNrsp reporter.
178
179 After confirming overexpression of ETV7 at the protein level (**Fig. 2D**), we verified the
180 inhibitory effects of ETV7 were not restricted to the reporter plasmid. We collected mRNA
181 and protein from IFN-α stimulated ETV7 overexpression cells to quantify effects on the
182 expression of endogenous ISGs. ETV7 overexpression significantly repressed the
183 induction of three prototypical ISGs (IFIT1, MX1, and ISG15) at the RNA level (**Fig. 2E**).
184 The reduction of ISG expression during ETV7 overexpression was also demonstrated at
185 the protein level for IFIT1 (**Fig. 2F**). These experiments show that overexpression of ETV7
186 is sufficient to repress ISG induction by type I IFN.
187

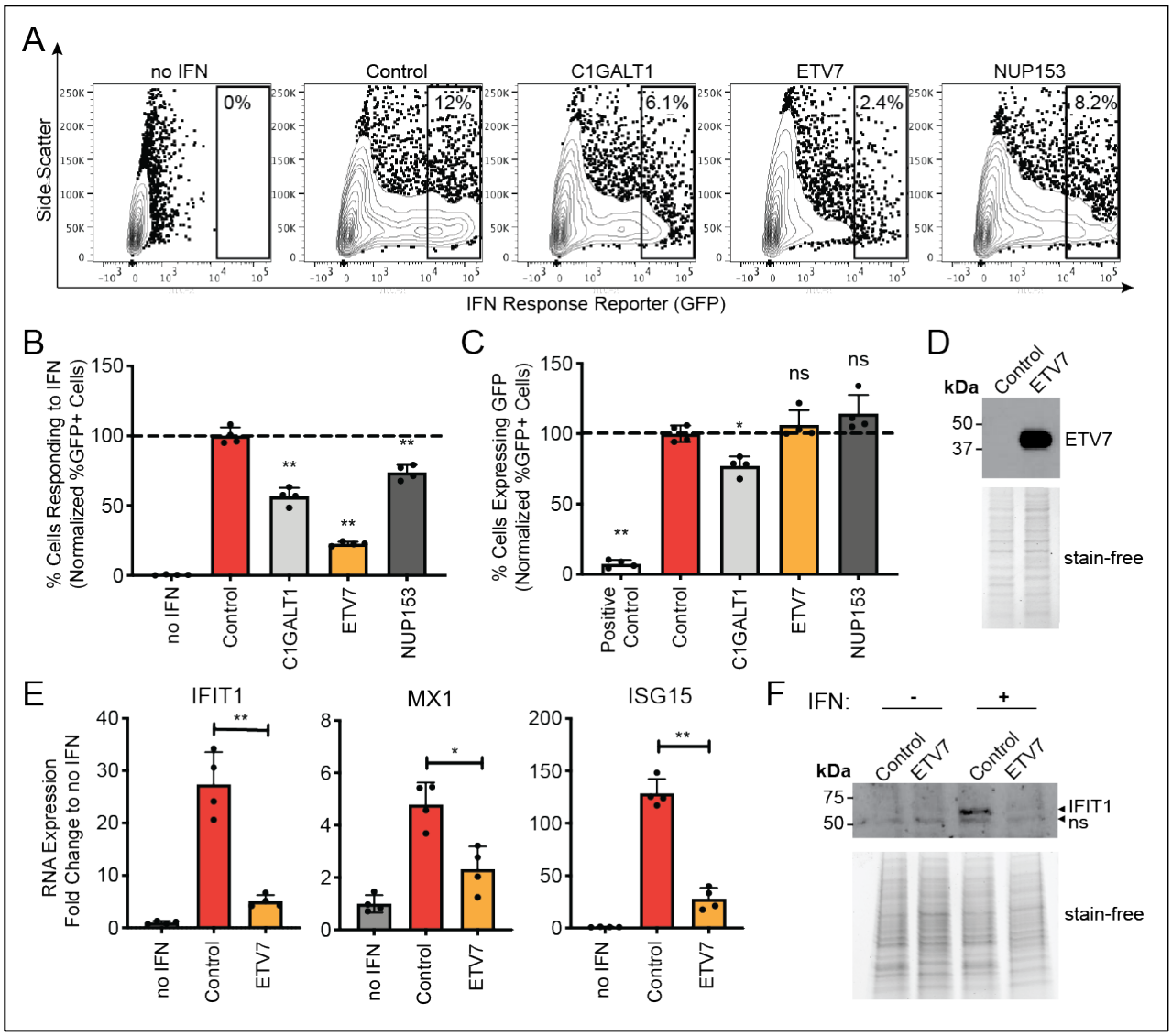

Fig. 2. ETV7 overexpression suppresses ISG expression. A) Flow cytometry plots of 293T cells transfected with the IFNrsp reporter and overexpression plasmids for the indicated screen hits then treated with IFN-α (100 U/mL, 6 h). B) Quantification of A showing normalized percentage of cells expressing GFP compared to the mCherry-expressing control (data shown as mean ± SD, n=4). C) Normalized percentage of cells expressing GFP from a constitutively expressing plasmid in cells overexpressing the indicated genes (positive control = EIF2AK1/HRI, shuts off translation) compared to control (data shown as mean ± SD, n=4). D) Western blot showing ETV7 protein levels in 293T cells transfected with the ETV7 overexpression plasmid. Stain-free gel imaging was used to confirm equal loading. E) Endogenous ISG mRNA expression levels measured using RT-qPCR after IFN-α treatment (100 U/mL, 9 h) (data shown as mean ± SD, n=4). F) Western blot comparing IFIT1 protein levels in control and ETV7 overexpressing cells after IFN-α treatment (500 U/mL, 18 h). ns = nonspecific band. Stain-free gel imaging was used to confirm equal loading. For all panels: Data shown are representative of two independent experiments. P-values calculated using unpaired, two-tailed Student's t-tests (*p<0.05, **p<0.001) compared to IFN-stimulated, mCherry-expressing control samples.

188

189 <u>ETV7 acts as a transcription factor to repress the type I IFN response.</u>

190 ETV7 is known to be a repressive transcription factor (26, 27), although a role in
191 repressing type I IFN responses has never been reported. To determine whether ETV7
192 acts as a transcription factor in this context, we generated a previously validated mutant
193 of ETV7, called ETV7(KALK), which is unable to bind DNA (**Fig. 3A and B**) (28).
194 Overexpression of ETV7(KALK) and stimulation with IFN-α had no measurable effect on
195 expression of the IFNrsp reporter, in contrast to WT ETV7 overexpression (**Fig. 3C**).

196

197 ETV7 has been reported to bind the canonical ETS family DNA motif, GGAA (29), known
198 as an "ETS" site (**Fig. 3D**). Since consensus ISREs can either contain or lack a GGAA
199 motif (**Supplementary Table 2**), we hypothesized ETV7 could act on specific ISGs based
200 on the presence of ETS sites in their promoters. The original IFN response reporter design
201 contained multiple ETS sites (**Fig. 3E**), which potentially explains why it is negatively
202 impacted by ETV7. To test the requirements of ETS sites for ETV7 repressive activity, we
203 generated an IFN response reporter containing seven consensus ISREs from canonical
204 ISGs that all lack ETS sites (ISRE -ETS) (**Fig. 3E**). We transfected the two reporter
205 plasmids (ISRE +ETS and ISRE -ETS) independently into 293T cells and stimulated with
206 IFN-α. As expected, both reporter plasmids responded to IFN treatment, but the
207 repressive activity of ETV7 was restricted to the reporter plasmid containing ETS motifs
208 (**Fig. 3F**). These experiments together demonstrate that ETV7's repressive activity
209 requires both its ability to bind DNA and the presence of ETS sites in ISG promoters.

210

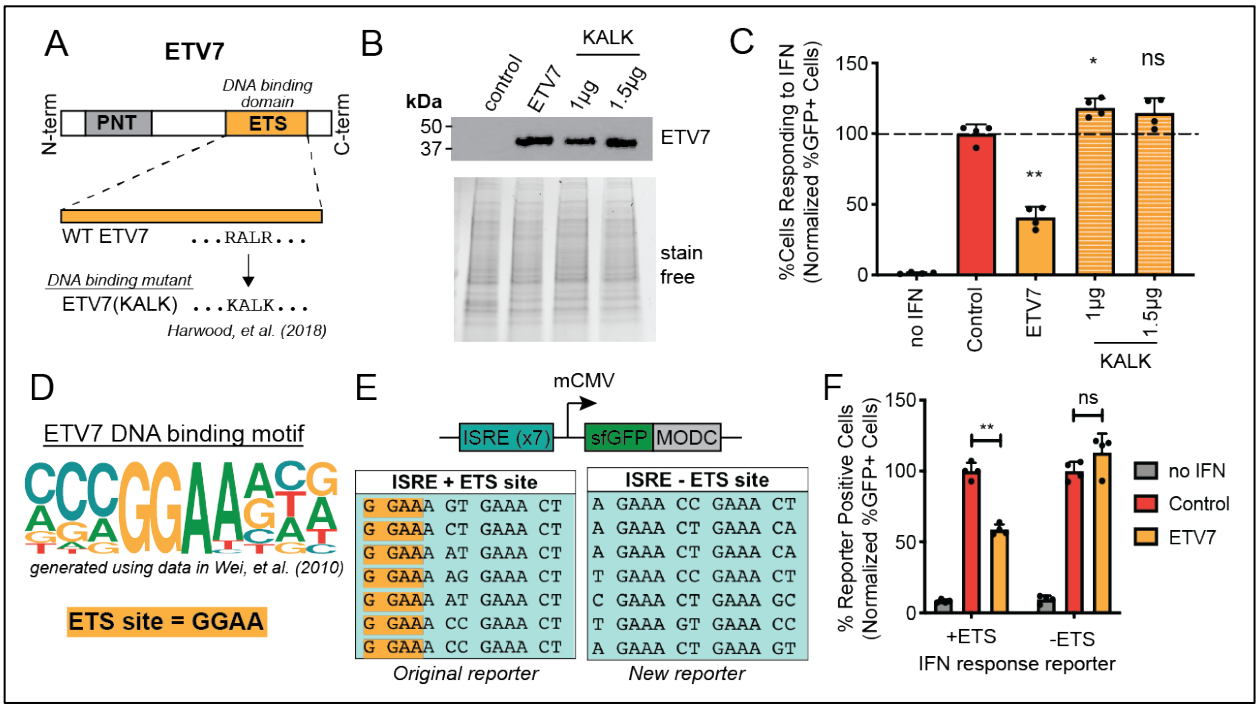

Fig. 3. ETV7 acts as a transcription factor to negatively regulate the type I IFN response. A) Diagram showing the ETV7 protein domains and amino acid changes made to generate the DNA binding mutant, ETV7(KALK). B) Western blot showing ETV7 protein levels in 293T cells transfected with WT (1μg) or DNA binding mutant (KALK) ETV7 expression plasmids. Stain-free gel imaging was used to confirm equal loading. C) Normalized percentage of 293T cells expressing GFP from the IFNrsp reporter with overexpression of WT or DNA binding mutant (KALK) ETV7 after IFN-α treatment (100 U/mL, 6 h) compared to control (data shown as mean ± SD, n=4, statistical analysis relative to IFN-stimulated, mCherry-expressing control samples). D) ETV7's DNA binding position weighted matrix (PWM) generated using enoLOGOS (69) with data from Wei et al. (70) and the conserved ETS family binding site, GGAA, highlighted in yellow. E) Diagrams of the IFNrsp reporters containing (+ETS) and not containing (-ETS) potential ETV7 binding sites (ETS site, highlighted in yellow). F) Normalized percentage of 293T cells expressing GFP from IFNrsp reporters either containing or not containing ETS sites after overexpression of ETV7 and IFN-α treatment (100 U/mL, 6 h) compared to mCherry-expressing control (data shown as mean ± SD, n=4). For all panels: Data shown are representative of two independent experiments. P-values calculated using unpaired, two-tailed Student's t-tests (*p<0.05, **p<0.001).

211 <u>ETV7 differentially regulates genes based on their ISRE sequence.</u>

212 Our data suggested ETV7 likely does not affect all ISG promoters. To perform an
213 unbiased examination of ETV7's repressive activity against ISGs with a variety of
214 potential regulatory sites, we performed RNA sequencing in cells with or without ETV7

overexpression and IFN stimulation (**Supplementary Data 3**). We then generated a dendrogram using the 2,000 most differentially expressed genes after IFN treatment to compare the four conditions: overexpression of control protein (mCherry) or ETV7, and with or without IFN-α treatment. When comparing the impact of IFN treatment on control and ETV7-overexpressing cells, we observed a larger divergence in the transcriptional profile of control cells compared to ETV7-overexpressing cells after IFN treatment (**Fig. 4A**). This difference demonstrates that ETV7 generally "dampens" the transcriptional impact of IFN treatment. Using a heat map to observe patterns in genes that increased at least two-fold upon IFN treatment, we found some genes are more suppressed during ETV7 overexpression than others (**Fig. 4B**). We divided these genes into three groups (from I = most affected to III = least affected) depending on their response to ETV7 overexpression and we examined their promoters to identify motifs associated with ETS transcription factors and IFN regulation. Unexpectedly, comparing the number of ETS binding sites (GGAA) across these three groups revealed no significant difference between the differentially affected groups (**Fig. 4C**). However, it is known that ETS sites sometimes occur as a part of combined motif related to ISREs, known as ETS-IRF combined elements (EICEs) with the consensus sequence GGAANN(N)GAAA (30, 31). We therefore tested the hypothesis that ETV7 negatively regulates ISGs with EICE sites. The number of EICE sites was significantly different between the most and least ETV7-affected groups (**Fig. 4D**), indicating ETV7 impacts the expression of specific ISGs by targeting an extended DNA binding motif.

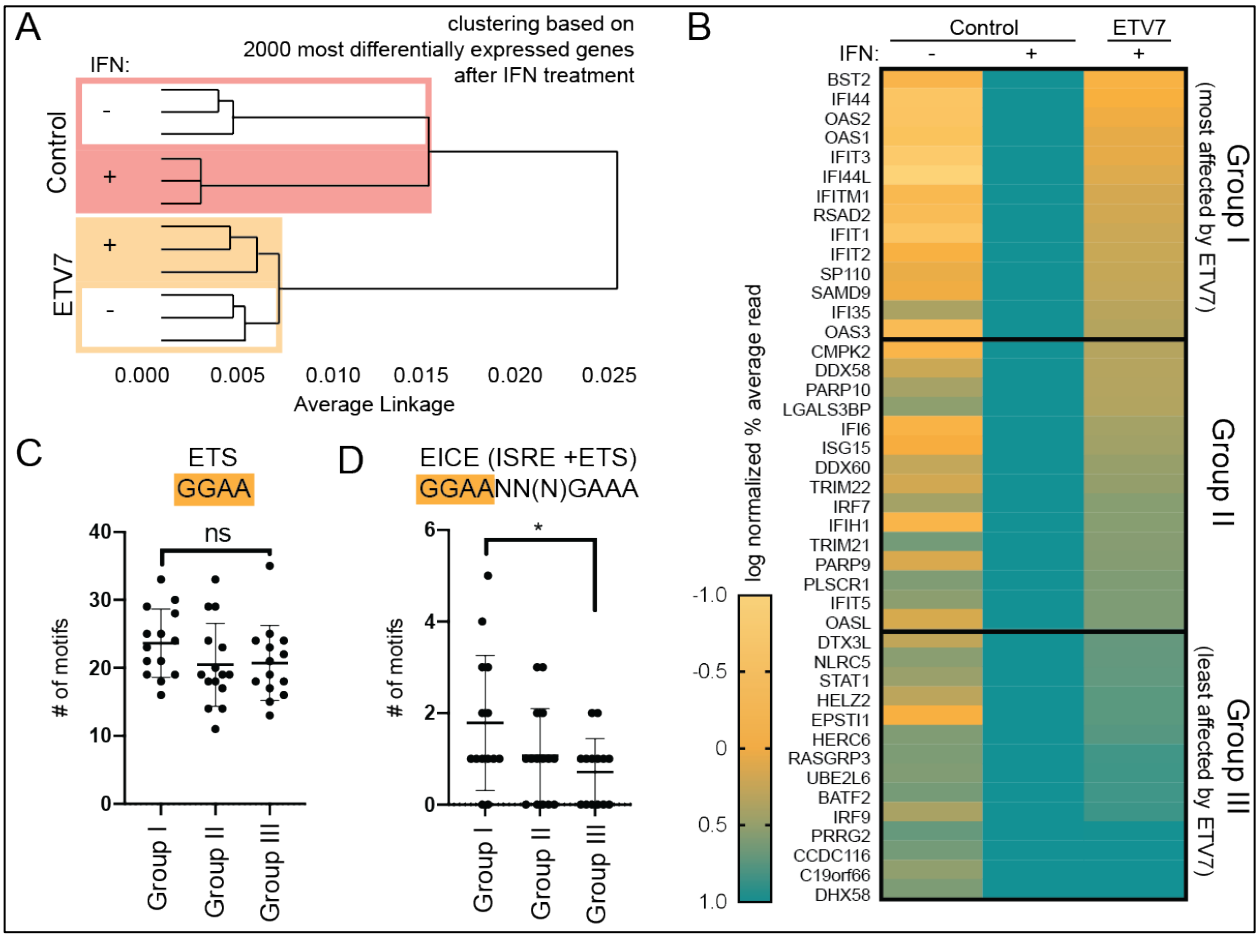

Fig. 4. ETV7 differentially regulates ISGs during the type I IFN response based on ISRE-related regulatory elements. A) Dendrogram of genes most differentially expressed in cells overexpressing either a control protein (mCherry) or ETV7 before and after IFN-α treatment (100 U/mL, 9 h) as measured using RNA sequencing. Three independent, biological replicates per condition. Red box highlights control samples, yellow box highlights ETV7-expressing samples, shading indicates IFN-stimulated samples. The box width indicates the linkage distance between samples before and after IFN, indicating control cells' transcriptional profile is more diverged after IFN treatment compared to ETV7-expressing cells. B) Heat map displaying RNA levels of genes upregulated at least two-fold following IFN-α treatment (100 U/mL, 9 h) in control cells. Expression was normalized to control cells after IFN treatment (averaged across replicates). Yellow = downregulated, blue = upregulated. C,D) Motif counts in promoter regions (-1000 bp, +500 bp) for the genes most and least affected by ETV7 overexpression in the RNA sequencing results. ETS sites (GGAA) highlighted in yellow. P-values calculated using unpaired, two-tailed Mann-Whitney U tests (*p<0.05, **p<0.001).

238

239

240 <u>ETV7 is required to negatively regulate specific ISGs.</u>

241 Our experiments to this point used an overexpression system to demonstrate that ETV7
242 is sufficient to suppress ISG expression. However, this approach leads to constitutive
243 ETV7 expression at high levels relative to the physiological magnitude and IFN-induced
244 expression of ETV7 (**Fig. 5A**). To determine the importance of ETV7 induction during the
245 IFN response, we performed a series of loss of function experiments that we expected
246 would have the reciprocal effect on IFN responses (32). We transduced A549-IFNrsp
247 reporter cells (the original reporter with ISRE +ETS sites) with Cas9 and one of two
248 different sgRNAs targeting ETV7 (ETV7 KO1, ETV7 KO2), selected for edited cells, and
249 then stimulated with IFN-α. Both guides resulted in significantly more IFN-induced sfGFP
250 expression compared to a control sgRNA (**Fig. 5B**). We next generated clonal ETV7
251 knockout A549 lung epithelial cell lines and sequenced the resulting DNA lesions to
252 confirm ETV7 knockout (**Supplementary Figure 2**). Since ETV7 is normally only
253 expressed after IFN stimulation, we treated with IFN-α and verified a reduction in ETV7
254 expression at the RNA level (**Fig. 5C**). We then selected five ISGs for RT-qPCR analysis.
255 Three (IFI44L, RSAD2/Viperin, IFIT3) were from the group most affected by ETV7 (Group
256 I) that contained multiple EICEs in their promoters. Two (IFIT5, IRF9) were chosen from
257 the less affected groups (Groups II and III). The EICE-rich genes (Group I) showed
258 significantly higher levels of RNA expression in the ETV7 knockout cells (**Fig. 5D**), while
259 genes with few EICEs were not significantly impacted by the loss of ETV7 (**Fig. 5E**). Thus,
260 the physiological level of ETV7 induction after IFN stimulation affects the expression of a
261 subset of ISGs.
262

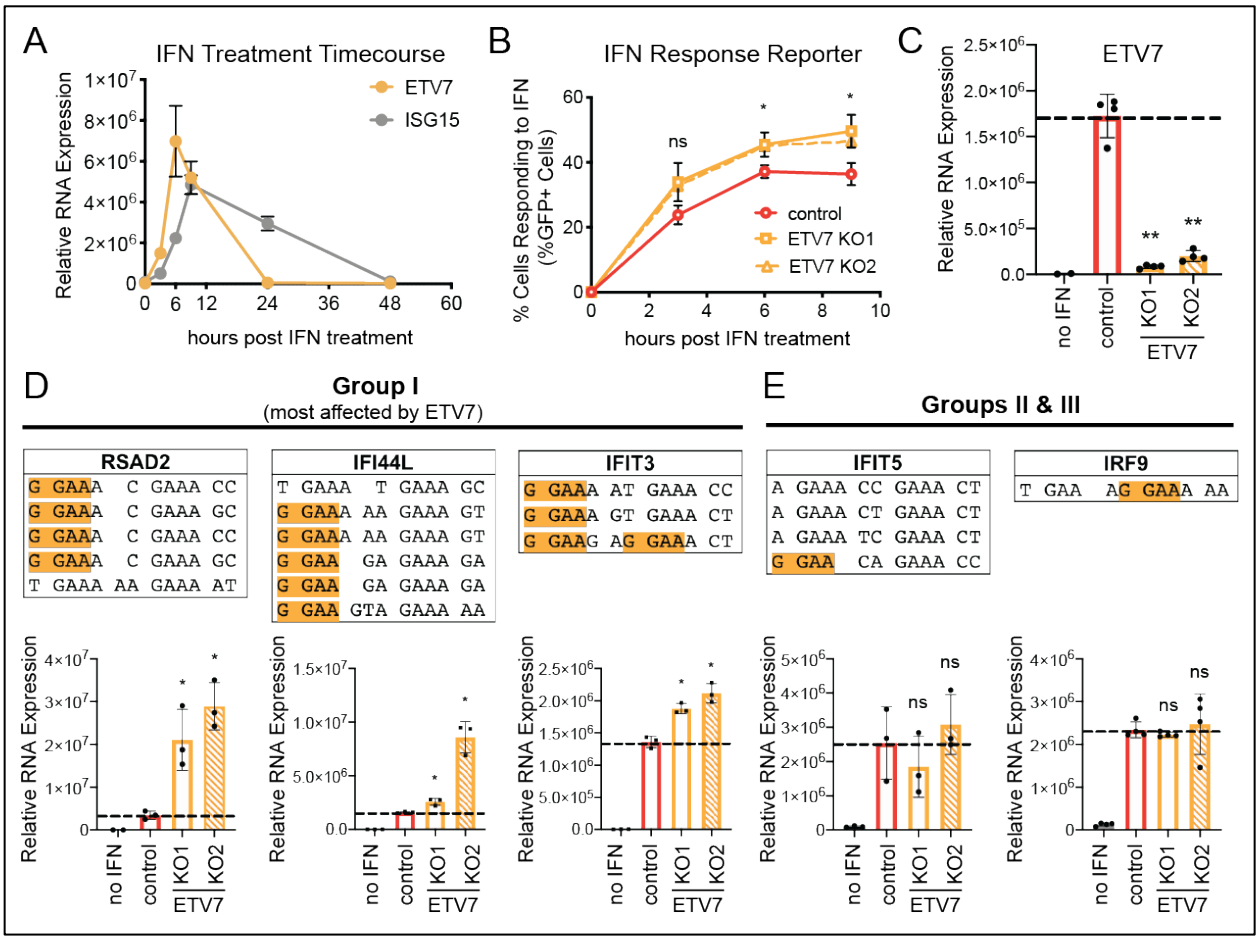

Fig. 5. ETV7 loss enhances expression of specific ISGs. A) ISG15 and ETV7 mRNA levels in A549 lung epithelial cells after IFN-α treatment (1000 U/mL, 6 h) (data shown as mean ± SD, n=4). B) Percentage of A549 cells expressing GFP from IFNrsp reporter after knockout of ETV7 and IFN-α treatment (1000 U/mL, 6 h) (data shown as mean ± SD, n=3, statistical analysis represents p-values for both of the two ETV7 KO sgRNAs compared to a non-targeting control). C) mRNA levels of ETV7 in non-targeting control and ETV7 KO A549 cells after IFN-α treatment (1000 U/mL, 6 h) (data shown as mean ± SD, n=4). D,E) Representative genes were chosen from the groups D) most affected by ETV7 (Group I) and E) least affected (Groups II and III) in the RNA sequencing analysis (**Fig. 4B**). Each gene's potential ISRE sequences (ETS sites highlighted in yellow) are shown, along with its mRNA levels in control and ETV7 KO cells after IFN-α treatment (1000 U/mL, 6 h) (data shown as mean ± SD, n=4). For all panels: Data shown are representative of two independent experiments. P-values calculated using unpaired, two-tailed Student's t-tests (*p<0.05, **p<0.001) compared to IFN-stimulated, non-targeting sgRNA control samples unless otherwise indicated.

263 <u>Loss of ETV7 restricts influenza viral replication.</u>

264 For a successful antiviral response, individual ISGs are thought to work together to restrict

265 multiple parts of the virus replication cycle (1). To determine whether the effects of ETV7

266 suppression of ISG expression were relevant in the context of a viral infection, we wanted
267 to identify a virus restricted by the genes regulated by ETV7 (i.e. Group I genes) (33).
268 Considering the Group I genes with well recognized antiviral functions (IFITM1, IFIT1-3,
269 OAS1-3, BST2, RSAD2), we found each had been reported to play important roles in the
270 restriction of influenza viruses (34). IFITM1 has been shown to prevent viral entry (35),
271 OAS proteins activate RNase L to degrade viral RNA (36), IFITs bind viral RNA and
272 promote antiviral signaling (37), and BST2/Tetherin and RSAD2/Viperin restrict viral
273 budding and egress (38, 39).
274
275 To determine whether ETV7 regulation affected influenza virus infection, we first infected
276 our ETV7 knockout A549 cells with a laboratory-adapted H1N1 influenza A virus (IAV),
277 A/Puerto Rico/8/1934 (PR8). Using a hemagglutination (HA) assay to measure the
278 number of viral particles released over time, we observed reduced virus production in our
279 ETV7 KO cells compared to control cells (**Fig. 6A**). This was the anticipated outcome
280 because loss of a negative regulator (i.e. ETV7) is expected to enhance expression of
281 antiviral ISGs. We also measured infectious viral titers and found a significant reduction
282 in our ETV7 KO cells compared to control cells (**Fig. 6B**). Using a fluorescent reporter
283 strain of PR8 (PR8-mNeon) (40), we next visualized infection and spread. As expected,
284 we observed fewer cells expressing mNeon in ETV7 KO cells using both microscopy (**Fig.
285 6C**) and flow cytometry readouts (**Fig. 6D**). Next, we tested whether ETV7's impact on
286 influenza virus infection and spread would extend to a more contemporary H1N1 IAV
287 strain, A/California/07/2009 (Cal/09), as well as an unrelated Victoria lineage influenza B
288 virus strain, B/Malaysia/2506/2004 (Mal/04) (41). Using these fluorescent reporter

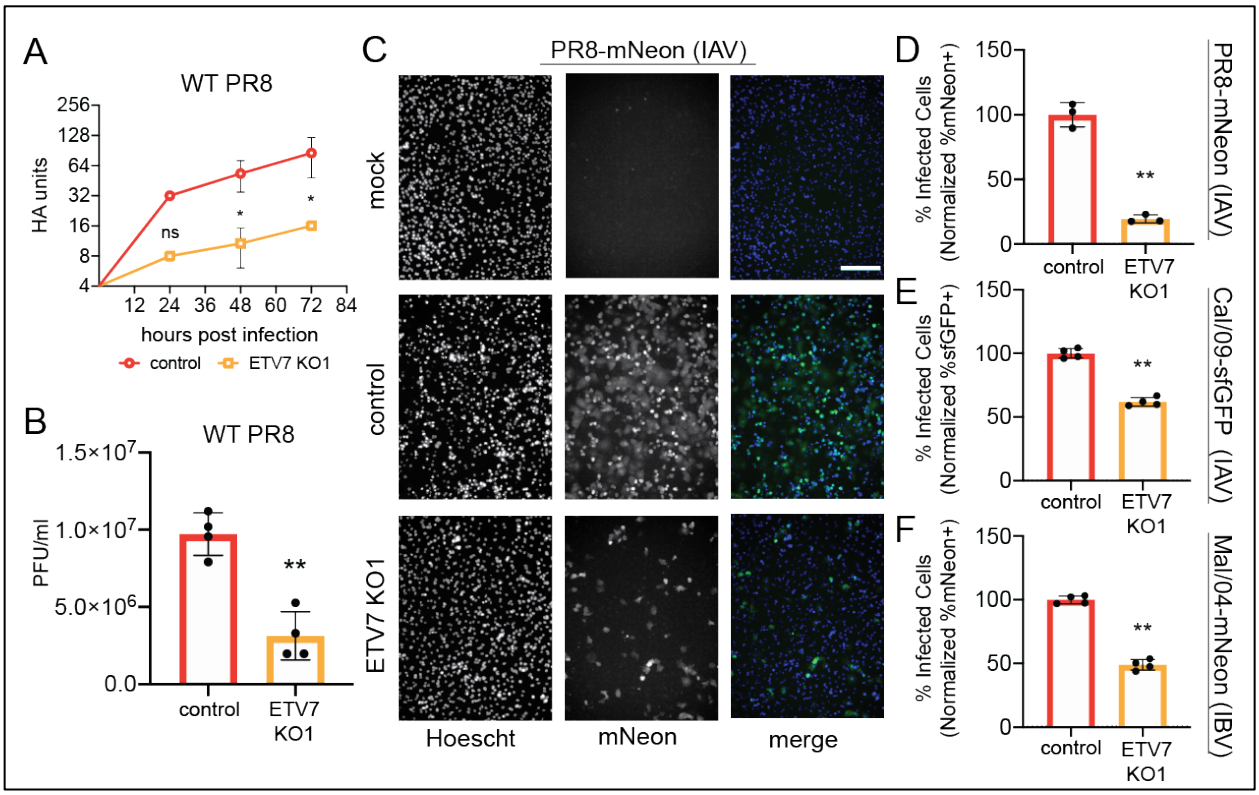

Fig. 6. Loss of ETV7 limits replication of multiple influenza viruses. A) Hemagglutination (HA) assay of virus collected at indicated time points from non-targeting control and ETV7 KO A549 cells after infection with WT PR8 virus (MOI=0.05, multicycle infection) (data shown as mean ± SD, n=3). B) Titer of virus collected from control and ETV7 KO A549 cells after infection with WT PR8 virus (18 h, MOI=0.05, multicycle infection) (data shown as mean ± SD, n=4). C) Control or ETV7 KO A549 cells after mock or PR8-mNeon reporter virus infection (24 h, MOI=0.1, multicycle infection). Green = mNeon, blue = nuclei. Scale bar, 200 µm. D) Flow cytometry quantification of control or ETV7 KO A549 cells after infection with PR8-mNeon reporter virus (24 h, MOI=0.01, multicycle infection) (data shown as mean ± SD, n=3). E,F) Normalized percentage of infected (reporter+) cells in ETV7 KO A549 cells compared to control cells after infection with E) Cal/09-sfGFP or F) Mal/04-mNeon reporter viruses (24 h, multicycle infection) (data shown as mean ± SD, n=4). For all panels: Data shown are representative of two independent experiments. P-values calculated using unpaired, two-tailed Student's t-tests (*p<0.05, **p<0.001) compared to influenza infected, non-targeting sgRNA control samples.

289 viruses, we observed significant decreases in the number of Cal/09- and Mal/04-infected

290 cells when comparing ETV7 KO cells to control cells (**Fig. 6E and F**). These experiments

291 demonstrate that loss of ETV7 leads to decreased viral replication across multiple,

292 unrelated influenza viruses.

Discussion

In this study, we performed a CRISPR activation screen to identify negative regulators of the type I IFN response. Specifically, we were interested in negative regulators that contribute to the types of differentiated ISG profiles IFN-induced activators are reported to produce. From this screen, we identified ETV7 as a negative IFN regulator and showed it acts as a transcription factor to repress subsets of ISGs dependent on a motif related to the ISRE, the EICE. We also showed ETV7's regulatory activity impacts the replication and spread of multiple strains of influenza viruses. These findings demonstrate the importance of ETV7 in fine-tuning the IFN response through specificity and transcriptional repression to regulate particular, antiviral ISG targets.

ETV7 is a member of the ETS family of transcription factors. This family performs diverse functions despite recognizing the same core DNA sequence, GGAA, by acting on extended motifs requiring binding partners (42, 43). In our work we identified the EICE, a recognized ETS transcription factor-associated motif, as a regulatory element related to ISREs that ETV7 uses to discriminate genes for regulation. The EICE has previously been reported to require an IRF binding partner to direct ETS transcription factor activity (30, 31); therefore, it is likely ETV7 has an IRF binding partner. If ETV7 does require a binding partner, this protein's induction and distribution likely contribute to the timing, gene targets, and activity of ETV7 during the IFN response. It is known that IRFs can be basally expressed (IRF2, IRF3) or IFN-induced (IRF1, IRF7) (44) and the availability of a binding partner could dramatically affect the timing and magnitude of effects on EICE-controlled ISGs. Future work will define if ETV7 has specific binding partners and how those

316 interactions may contribute to the nonuniform, repressive activity of ETV7 during the type
317 I IFN response reported in this study.
318
319 IFN-induced regulators control the magnitude and duration of IFN responses in addition
320 to the temporal regulation of specific waves of ISGs (45). These coordinated waves of
321 ISG induction can peak early or late during the IFN response and are thought to
322 correspond to specific stages of virus replication or immune processes (1, 6). We
323 compared the induction of ETV7 and ISG15 and observed ETV7 is both upregulated and
324 downregulated at earlier time points than this prototypical ISG (**Fig. 5A**). We expanded
325 our analysis to published datasets of human gene expression during respiratory infections
326 and concluded that ETV7 is generally induced earlier than many ISGs (46). Although not
327 the focus of our study, ETV7's early and short induction pattern suggests it may be a key
328 regulator of the first stages of IFN-mediated gene induction. We favor a model wherein
329 early ETV7 expression is responsible for reducing the accumulation, or delaying the
330 expression, of ISGs controlled by EICE motifs (**Supplementary Fig. 3**).
331
332 ETV7 is induced during infections across many vertebrate species (47, 48), indicating a
333 potential conserved, relevant role in the immune response; however, ETV7 has been lost
334 in mice and closely related rodents (49). Since mice and rodents have an intact interferon
335 response pathway, a natural question is: how are the activities of ETV7 being accounted
336 for in these animals? While we have no clear answer from the data in this study, it is well-
337 recognized that IFN responses contains many redundancies (33). Accordingly, we believe
338 other ETS family members, potentially the closely related ETV6 (which is also induced by

339 IFNs), may perform the role of ETV7 in mice (50). Future studies will be required to test
340 the hypothesis that mice induce an ETV7-related alternative during the type I IFN
341 response.
342
343 Another important question is why ETV7's IFN-induced activity has been maintained
344 throughout evolution. In this report, we provide evidence that ETV7's activity reduces a
345 cell's ability to restrict influenza virus infection; this seems counterintuitive to ETV7
346 benefitting the host. We hypothesize that regulators like ETV7 are important to prevent
347 excessive inflammatory signaling. It is appreciated that negative regulators of the IFN
348 response are required to prevent extreme and prolonged immune responses, which are
349 associated with poor disease outcomes after infection (51–53). ETV7 potentially
350 contributes to the cumulative activities of negative IFN regulators to limit IFN responses
351 during pathogen clearance. Additionally, it stands to reason that different individual ISGs
352 have differing toxic effects on the cell. It is tempting to speculate that ETV7 suppresses
353 ISGs whose accumulation is particularly harmful to cell viability and host recovery after
354 infection.
355
356 Additionally, the relevance of controlled IFN responses goes beyond infectious disease;
357 patients with dysfunctional USP18, a negative regulator of the IFN response, develop a
358 type I interferonopathy that results in a severe pseudo-TORCH syndrome (54). Mouse
359 knockouts for other negative regulators of the IFN response (SOCS1, SOCS3, USP18)
360 also develop non-pathogen associated, chronic inflammatory diseases (55–58). ETV7's
361 lack of murine homolog eliminates an easily generated animal-knockout model to

experimentally show ETV7's relevance as a general innate immune repressor. However, genome wide association studies (GWAS) have linked ETV7 to autoimmune diseases including rheumatoid arthritis and multiple sclerosis (59, 60); both of these autoimmune diseases have evidence of enhanced ISG expression (61, 62). Thus, although the specific contributions of ETV7 activity to IFN regulation are currently undefined, its potential role is not limited to viral infections.

In conclusion, we identified ETV7 as a negative regulator of the type I IFN response. Previously, ETV7 was appreciated to be an ISG; however, a specific function during the IFN response was unknown. We determined that ETV7 acts as a transcription factor to target specific ISGs for repression, potentially contributing to the complex ISG transcriptional landscape. Additionally, many of the ETV7-modulated ISGs restrict influenza viruses (34) and we showed that loss of ETV7 limits influenza virus spread. Further work is required to understand the complexity of IFN regulation, while therapeutic targeting of factors like ETV7 could lead to the development of a new class of host-directed antivirals that tailor ISG responses to specific viruses.

378 **Experimental Procedures**

379 **Cloning**

380 To generate reporters sensitive to IFN, we designed gBlocks (IDT) containing ISREs to
381 be cloned into the pTRIP vector ahead of a minimal CMV promoter controlling expression
382 of sfGFP. To clone and express the open reading frames (ORFs) of our screen hits, we
383 designed primers for cloning into the pLEX-MCS vector using Gibson Assembly (NEB).
384 To amplify ETV7 and NUP153, we used cDNA templates from Transomic Technologies.
385 To amplify C1GALT1 and EIF2AK1, we used RNA from IFN-stimulated A549 cells. The
386 DNA binding mutant, ETV7(KALK) (28), was also generated using a gBlock. Non-
387 targeting and ETV7-targeting CRISPR KO sgRNAs were cloned by annealing oligos
388 encoding the desired sgRNA sequence and ligating them directly into the lentiCRISPRv2
389 vector (Addgene). DNA was transformed into NEB 5-alpha high efficiency competent
390 cells. Insert size was verified with PCR and purified plasmids were sequenced using
391 Sanger sequencing.

392

393 **Cells**

394 All cells were obtained from ATCC and grown at 37°C in 5% CO_2. A549 and 293T cells
395 were grown in Dulbecco's Modified Eagle Medium (DMEM) supplemented with 5% fetal
396 bovine serum, GlutaMAX, and penicillin-streptomycin. Madin-Darby canine kidney
397 (MDCK) cells were grown in minimal essential media (MEM) supplemented with 5% fetal
398 bovine serum, HEPES, $NaHCO_3$, GlutaMAX, and penicillin-streptomycin. The A549
399 CRISPR-SAM cells were previously validated (63) and transduced with the IFNrsp

400 reporter three times before being clonally selected. The A549 CRISPR KO cells were
401 transduced and then selected using puromycin (10 μg/mL).
402
403 **Flow Cytometry**
404 Cells were trypsinized and analyzed on a Fortessa X-20 (BD) machine with standard laser
405 and filter combinations. Data was visualized and processed with FlowJo software.
406
407 **CRISPR Activation Screen**
408 The sgRNA library was packaged into lentivirus as previously described (63). After
409 packaging and titering the lentivirus, $2x10^8$ A549-CRISPR-SAM-IFNresp cells were
410 seeded onto 15 cm plates (10 plates total). The next day they were transduced with the
411 packaged sgRNA library (MOI=0.5). After 48 h, the transduced cells were split and half
412 were collected as a transduction control, while the remaining half were plated back onto
413 15 cm plates. The next day, cells were treated with IFN-α ($4x10^3$ U/mL) for 6 h. Cells were
414 then collected and sorted on a Beckman Coulter Astrios cell sorter. Specifically, gates
415 were set to sort GFP-negative cells as the population of interest, as well as GFP-positive
416 cells as a control population of cells still capable of signaling. This screen was performed
417 in duplicate. Genomic DNA was extracted from sorted cells using the Zymo Quick gDNA
418 micro prep kit. PCR was subsequently performed using barcoded primers as previously
419 described using the NEB Next High Fidelity 2x PCR master mix (63). PCR bands were
420 gel purified using the Thermo GeneJET gel extraction kit. Samples were then sequenced
421 via next-generation Illumina MiSeq using paired-end 150 bp reads.
422

423 **Screen Analysis**

424 Raw MiSeq read files were aligned to the CRISPR SAM sgRNA library and raw reads for
425 each sgRNA were counted using the MAGeCK pipeline (22). sgRNA enrichment was
426 determined using the generated count files and the MAGeCK-MLE analysis pipeline.
427 Genes were sorted based on z-score and determined to be significantly enriched if their
428 z-score was at least two standard deviations above the average z-score of the entire
429 sorted population.

430

431 **Western Blotting**

432 Cells were trypsinized and $1x10^6$ cells were pelleted at 800 x g for 5 min. Equal amounts
433 of cellular material were loaded into 4-20% acrylamide gels (Bio-Rad) and imaged using
434 a ChemiDoc Imaging System (Bio-Rad). Protein was transferred to a nitrocellulose
435 membrane at 60V for 60 min. PBS with 5% (w/v) non-fat dried milk and 0.1% Tween-20
436 were used to block for 1 h at 4°C. Primary antibodies were then incubated with the
437 membrane overnight at 4°C. Antibodies used were rabbit anti-ETV7 (Sigma, HPA029033)
438 and rabbit anti-IFIT1 (Cell Signaling, D2X9Z). Membranes were washed five times in PBS
439 with 0.1% Tween-20 and then an anti-rabbit-HRP secondary antibody (Thermo, A16104)
440 was added for 1 h. The membrane was then washed five times and Clarity or Clarity Max
441 ECL substrate (Bio-Rad) was added before being exposed to film and developed.

442

443 **RT-qPCR**

444 Total RNA was collected using Monarch Total RNA Miniprep Kits (NEB). One-step RT-
445 qPCR was performed with commercial TaqMan assays from Thermo for ETV7

446 (Hs00903229_m1), C1GALT1 (Hs00863329_g1), NUP153 (Hs01018919_m1), ISG15
447 (Hs00196051_m1), MX1 (Hs00895608_m1), IFIT1 (Hs00356631_g1), RSAD2
448 (Hs00895608_m1), IFI44L (Hs00915292_m1), IFIT3 (Hs01922752_s1), IFIT5
449 (Hs00202721_m1), and IRF9 (Hs00196051_m1) using the EXPRESS One-Step
450 Superscript qRT-PCR Kit on an Applied Biosystems StepOnePlus instrument. RNA was
451 normalized using an endogenous 18S rRNA primer/probe set (Applied Biosystems).
452

453 **RNA sequencing**

454 293T cells were transfected with ETV7- or control-expressing plasmids and selected
455 using puromycin (20 μg/mL) for 24 h before treatment with IFN-α (100 U/mL). Total RNA
456 was collected at 9 h post-IFN treatment using Monarch Total RNA Miniprep Kits (NEB).
457 RNA was prepped for RNA sequencing submission using the NEBNext Poly(A) mRNA
458 Magnetic Isolation Module (NEB), NEBNext Ultra II RNA Library Prep Kit for Illumina
459 (NEB), and NEBNext Multiplex Oligos for Illumina (NEB). Samples were analyzed on one
460 lane of an Illumina HiSeq 4000 using 50 bp single strand reads. Mapping of the raw reads
461 to the human hg19 reference genome was accomplished using a custom application on
462 the Illumina BaseSpace Sequence Hub (64). After data normalization, average read
463 values were compared across samples. For comparisons in which some samples had
464 zero reads detected for a specific gene, one read was added to all values in the sample
465 to complete analyses that required non-zero values. Dendrograms were generated by
466 identifying the 2,000 most differentially expressed genes in the control samples with and
467 without IFN treatment using a Student's t-test and plotted using Heatmapper (65). The
468 heat map shows genes upregulated 2-fold (after normalization) with IFN treatment in the

469 control samples. Values shown are log normalized to the control samples with IFN
470 treatment.
471
472 **Viruses**
473 PR8-mNeon was generated via insertion of the mNeon fluorescent gene (66) into
474 segment 4 of the virus (40). Mal/04-mNeon was generated by inserting the mNeon
475 fluorescent gene (66) into segment 4 of the Mal/04 genome (41). Cal/09-sfGFP was
476 generated via insertion of the sfGFP gene (67) into segment 8 of the virus using the same
477 scheme previously used to insert Cre recombinase (68). For influenza virus infections,
478 cells were either mock- or virus-infected for 1 h and then cultured in OptiMEM
479 supplemented with bovine serum albumin (BSA), penicillin-streptomycin, and 0.2 μg/mL
480 TPCK-treated trypsin protease (Sigma). PR8 WT, PR8-mNeon, Cal/09-sfGFP, and were
481 incubated at 37°C, Mal/04-mNeon was incubated ay 33°C.
482
483 **Viral Growth Assays**
484 Hemagglutination (HA) assays to measure the amount of viral particles were performed
485 by diluting influenza infected cell supernatants collected at the indicated time points in
486 cold PBS. An equal amount of chicken blood diluted 1:40 in PBS was mixed with serially
487 diluted virus and incubated at 4°C for 2-3 h before scoring. Infectious viral titers were
488 determined using standard plaque assay procedures on MDCK cells. Infected cell
489 supernatants were collected at 18 h, serially diluted, and used to infect confluent 6-well
490 plates for 1 h before removing the virus and adding the agar overlay. Cells were then
491 incubated at 37°C for 48 h before being fixed in 4% PFA overnight. The 4% PFA was then

492 aspirated, and the agar layer was removed before washing cells with PBS. Serum from
493 WT PR8 infected mice was diluted 1:2,000 in antibody dilution buffer (5% (w/v) non-fat
494 dried milk and 0.05% Tween-20 in PBS) and incubated on cells at 4°C overnight. Cells
495 were then washed twice with PBS and incubated for 1 h with anti-mouse IgG horseradish
496 peroxidase (HRP)-conjugated sheep antibody (GE Healthcare) diluted 1:4,000 in
497 antibody dilution buffer. Assays were then washed twice with PBS and exposed to 0.5 mL
498 of TrueBlue peroxidase substrate (KPL) for 20 min. Plates were then washed with water
499 and dried before plaques were counted.
500
501 **Data Availability**
502 All next generation sequencing data are available at NCBI GEO under accession number
503 GSE140718.
504
505

506 **References**
507

508 1. W. M. Schneider, M. D. Chevillotte, C. M. Rice, Interferon-Stimulated Genes: A
509 Complex Web of Host Defenses. *Annu. Rev. Immunol.* **32**, 513–545 (2014).
510 2. J. W. Schoggins, Interferon-Stimulated Genes: What Do They All Do? *Annu. Rev.*
511 *Virol.* **6**, 567–584 (2019).
512 3. J. W. Schoggins, *et al.*, A diverse range of gene products are effectors of the type
513 I interferon antiviral response. *Nature* **472**, 481–485 (2011).
514 4. J. W. Schoggins, *et al.*, Pan-viral specificity of IFN-induced genes reveals new
515 roles for cGAS in innate immunity. *Nature* **505**, 691–695 (2014).
516 5. M. Kane, *et al.*, Identification of Interferon-Stimulated Genes with Antiretroviral
517 Activity. *Cell Host Microbe* **20**, 392–405 (2016).
518 6. E. V. Mesev, R. A. LeDesma, A. Ploss, Decoding type I and III interferon
519 signalling during viral infection. *Nat. Microbiol.* **4**, 914–924 (2019).
520 7. G. R. Stark, J. E. Darnell, The JAK-STAT Pathway at Twenty. *Immunity* **36**, 503–
521 514 (2012).
522 8. K. Honda, H. Yanai, A. Takaoka, T. Taniguchi, Regulation of the type I IFN
523 induction: a current view. *Int. Immunol.* **17**, 1367–1378 (2005).
524 9. D. E. Levy, D. S. Kessler, R. Pine, N. Reich, J. E. Darnell, Interferon-induced
525 nuclear factors that bind a shared promoter element correlate with positive and
526 negative transcriptional control. *Genes Dev.* **2**, 383–93 (1988).
527 10. K.-I. Arimoto, S. Miyauchi, S. A. Stoner, J.-B. Fan, D.-E. Zhang, Negative
528 regulation of type I IFN signaling. *J. Leukoc. Biol.* **103**, 1099–1116 (2018).
529 11. H. Zheng, J. Qian, B. Varghese, D. P. Baker, S. Fuchs, Ligand-stimulated
530 downregulation of the alpha interferon receptor: role of protein kinase D2. *Mol.*
531 *Cell. Biol.* **31**, 710–20 (2011).
532 12. N. P. D. Liau, *et al.*, The molecular basis of JAK/STAT inhibition by SOCS1. *Nat.*
533 *Commun.* **9**, 1558 (2018).
534 13. M. P. Malakhov, O. A. Malakhova, K. Il Kim, K. J. Ritchie, D.-E. Zhang, UBP43
535 (USP18) specifically removes ISG15 from conjugated proteins. *J. Biol. Chem.*
536 **277**, 9976–81 (2002).
537 14. P. J. Hertzog, B. R. G. Williams, Fine tuning type I interferon responses. *Cytokine*
538 *Growth Factor Rev.* **24**, 217–225 (2013).
539 15. J. P. B. Viola, *et al.*, A Positive Feedback Amplifier Circuit That Regulates
540 Interferon (IFN)-Stimulated Gene Expression and Controls Type I and Type II IFN
541 Responses. **9**, 28 (2018).
542 16. N. Tanaka, T. Kawakami, T. Taniguchi, Recognition DNA sequences of interferon
543 regulatory factor 1 (IRF-1) and IRF-2, regulators of cell growth and the interferon
544 system. *Mol. Cell. Biol.* **13**, 4531–8 (1993).
545 17. M. Sato, *et al.*, Positive feedback regulation of type I *IFN* genes by the IFN-
546 inducible transcription factor IRF-7. *FEBS Lett.* **441**, 106–110 (1998).
547 18. L. L. Seifert, *et al.*, The ETS transcription factor ELF1 regulates a broadly antiviral
548 program distinct from the type I interferon response. *PLOS Pathog.* **15**, e1007634
549 (2019).
550 19. P. Hubel, *et al.*, A protein-interaction network of interferon-stimulated genes
551 extends the innate immune system landscape. *Nat. Immunol.* **20**, 493–502

552 (2019).
553 20. X. Li, *et al.*, Generation of Destabilized Green Fluorescent Protein as a
554 Transcription Reporter. *J. Biol. Chem.* **273**, 34970–34975 (1998).
555 21. S. Konermann, *et al.*, Genome-scale transcriptional activation by an engineered
556 CRISPR-Cas9 complex. *Nature* **517**, 583–8 (2015).
557 22. W. Li, *et al.*, MAGeCK enables robust identification of essential genes from
558 genome-scale CRISPR/Cas9 knockout screens. *Genome Biol.* **15**, 554 (2014).
559 23. I. Rusinova, *et al.*, INTERFEROME v2.0: an updated database of annotated
560 interferon-regulated genes. *Nucleic Acids Res.* **41**, D1040–D1046 (2012).
561 24. A.-P. Han, *et al.*, Heme-regulated eIF2alpha kinase (HRI) is required for
562 translational regulation and survival of erythroid precursors in iron deficiency.
563 *EMBO J.* **20**, 6909–6918 (2001).
564 25. A. Marg, *et al.*, Nucleocytoplasmic shuttling by nucleoporins Nup153 and Nup214
565 and CRM1-dependent nuclear export control the subcellular distribution of latent
566 Stat1. *J. Cell Biol.* **165**, 823–33 (2004).
567 26. M. D. Potter, A. Buijs, B. Kreider, L. van Rompaey, G. C. Grosveld, Identification
568 and characterization of a new human ETS-family transcription factor, TEL2, that is
569 expressed in hematopoietic tissues and can associate with TEL1/ETV6. *Blood* **95**,
570 3341–8 (2000).
571 27. H. Poirel, *et al.*, Characterization of a novel ETS gene, TELB, encoding a protein
572 structurally and functionaly related to TEL. *Oncogene* **19**, 4802–4806 (2000).
573 28. F. C. Harwood, *et al.*, ETV7 is an essential component of a rapamycin-insensitive
574 mTOR complex in cancer. *Sci. Adv.* **4**, eaar3938 (2018).
575 29. H. Wei, *et al.*, Genome-wide analysis of ETS-family DNA-binding in vitro and in
576 vivo. *EMBO J.* **29**, 2147–2160 (2010).
577 30. A. L. Brass, E. Kehrli, C. F. Eisenbeis, U. Storb, H. Singh, Pip, a lymphoid-
578 restricted IRF, contains a regulatory domain that is important for autoinhibition
579 and ternary complex formation with the Ets factor PU.1. *Genes Dev.* **10**, 2335–
580 2347 (1996).
581 31. D. Meraro, M. Gleit-Kielmanowicz, H. Hauser, B.-Z. Levi, IFN-Stimulated Gene 15
582 Is Synergistically Activated Through Interactions Between the
583 Myelocyte/Lymphocyte-Specific Transcription Factors, PU.1, IFN Regulatory
584 Factor-8/IFN Consensus Sequence Binding Protein, and IFN Regulatory Factor-4:
585 Characterization o. *J. Immunol.* **168**, 6224–6231 (2002).
586 32. N. E. Sanjana, O. Shalem, F. Zhang, Improved vectors and genome-wide libraries
587 for CRISPR screening. *Nat. Methods* **11**, 783–784 (2014).
588 33. J. W. Schoggins, Recent advances in antiviral interferon-stimulated gene biology.
589 *F1000Research* **7**, 309 (2018).
590 34. A. García-Sastre, Induction and evasion of type I interferon responses by
591 influenza viruses. *Virus Res.* **162**, 12–18 (2011).
592 35. A. L. Brass, *et al.*, The IFITM Proteins Mediate Cellular Resistance to Influenza A
593 H1N1 Virus, West Nile Virus, and Dengue Virus. *Cell* **139**, 1243–1254 (2009).
594 36. Y. Li, *et al.*, Activation of RNase L is dependent on OAS3 expression during
595 infection with diverse human viruses. *Proc. Natl. Acad. Sci. U. S. A.* **113**, 2241–6
596 (2016).
597 37. A. Pichlmair, *et al.*, IFIT1 is an antiviral protein that recognizes 5′-triphosphate

598 RNA. *Nat. Immunol.* **12**, 624–630 (2011).
599 38. M. A. Yondola, *et al.*, Budding capability of the influenza virus neuraminidase can
600 be modulated by tetherin. *J. Virol.* **85**, 2480–91 (2011).
601 39. X. Wang, E. R. Hinson, P. Cresswell, The Interferon-Inducible Protein Viperin
602 Inhibits Influenza Virus Release by Perturbing Lipid Rafts. *Cell Host Microbe* **2**,
603 96–105 (2007).
604 40. A. T. Harding, B. E. Heaton, R. E. Dumm, N. S. Heaton, Rationally Designed
605 Influenza Virus Vaccines That Are Antigenically Stable during Growth in Eggs.
606 *MBio* **8** (2017).
607 41. R. E. Dumm, *et al.*, Non-lytic clearance of influenza B virus from infected cells
608 preserves epithelial barrier function. *Nat. Commun.* **10**, 779 (2019).
609 42. R. Li, H. Pei, D. K. Watson, Regulation of Ets function by protein–protein
610 interactions. *Oncogene* **19**, 6514–6523 (2000).
611 43. A. Verger, M. Duterque-Coquillaud, When Ets transcription factors meet their
612 partners. *BioEssays* **24**, 362–370 (2002).
613 44. T. Taniguchi, K. Ogasawara, A. Takaoka, N. Tanaka, IRF Family of Transcription
614 Factors as Regulators of Host Defense. *Annu. Rev. Immunol.* **19**, 623–655
615 (2001).
616 45. W. Wang, L. Xu, J. Su, M. P. Peppelenbosch, Q. Pan, Transcriptional Regulation
617 of Antiviral Interferon-Stimulated Genes. *Trends Microbiol.* **25**, 573–584 (2017).
618 46. T.-Y. Liu, *et al.*, An individualized predictor of health and disease using paired
619 reference and target samples. *BMC Bioinformatics* **17**, 47 (2016).
620 47. P. C. De La Cruz-Rivera, *et al.*, The IFN Response in Bats Displays Distinctive
621 IFN-Stimulated Gene Expression Kinetics with Atypical RNASEL Induction. *J.*
622 *Immunol.* **200**, 209–217 (2018).
623 48. , Transcriptome and proteome profiling of host responses to Marek's disease virus
624 in chickens. *Vet. Immunol. Immunopathol.* **138**, 292–302 (2010).
625 49. H. Kawagoe, M. Potter, J. Ellis, G. C. Grosveld, TEL2, an ETS factor expressed in
626 human leukemia, regulates monocytic differentiation of U937 cells and blocks the
627 inhibitory effect of TEL1 on Ras-induced cellular transformation. *Cancer Res.* **64**,
628 6091–6100 (2004).
629 50. P. Rasighaemi, A. C. Ward, ETV6 and ETV7: Siblings in hematopoiesis and its
630 disruption in disease. *Crit. Rev. Oncol. Hematol.* **116**, 106–115 (2017).
631 51. J. A. Nick, *et al.*, Extremes of Interferon-Stimulated Gene Expression Associate
632 with Worse Outcomes in the Acute Respiratory Distress Syndrome. *PLoS One* **11**,
633 e0162490 (2016).
634 52. Y. Muramoto, *et al.*, Disease severity is associated with differential gene
635 expression at the early and late phases of infection in nonhuman primates
636 infected with different H5N1 highly pathogenic avian influenza viruses. *J. Virol.* **88**,
637 8981–97 (2014).
638 53. S. Davidson, M. K. Maini, A. Wack, Disease-promoting effects of type I interferons
639 in viral, bacterial, and coinfections. *J. Interferon Cytokine Res.* **35**, 252–64 (2015).
640 54. M. E. C. Meuwissen, *et al.*, Human USP18 deficiency underlies type 1
641 interferonopathy leading to severe pseudo-TORCH syndrome. *J. Exp. Med.* **213**,
642 1163–74 (2016).
643 55. J.-C. Marine, *et al.*, SOCS1 Deficiency Causes a Lymphocyte-Dependent

Perinatal Lethality. *Cell* **98**, 609–616 (1999).
56. W. S. Alexander, *et al.*, SOCS1 Is a Critical Inhibitor of Interferon γ Signaling and Prevents the Potentially Fatal Neonatal Actions of this Cytokine. *Cell* **98**, 597–608 (1999).
57. B. A. Croker, *et al.*, SOCS3 negatively regulates IL-6 signaling in vivo. *Nat. Immunol.* **4**, 540–545 (2003).
58. K. J. Ritchie, *et al.*, Dysregulation of protein modification by ISG15 results in brain cell injury. *Genes Dev.* **16**, 2207–12 (2002).
59. Y. Okada, *et al.*, Genetics of rheumatoid arthritis contributes to biology and drug discovery. *Nature* **506**, 376–381 (2014).
60. T. James, *et al.*, Impact of genetic risk loci for multiple sclerosis on expression of proximal genes in patients. *Hum. Mol. Genet.* **27**, 912–928 (2018).
61. J. E. Castañeda-Delgado, *et al.*, Type I Interferon Gene Response Is Increased in Early and Established Rheumatoid Arthritis and Correlates with Autoantibody Production. *Front. Immunol.* **8**, 285 (2017).
62. A. Hundeshagen, *et al.*, Elevated type I interferon-like activity in a subset of multiple sclerosis patients: molecular basis and clinical relevance. *J. Neuroinflammation* **9**, 574 (2012).
63. B. E. Heaton, *et al.*, A CRISPR Activation Screen Identifies a Pan-avian Influenza Virus Inhibitory Host Factor. *Cell Rep.* **20**, 1503–1512 (2017).
64. N. S. Heaton, *et al.*, Long-term survival of influenza virus infected club cells drives immunopathology. **211**, 1707–1714 (2014).
65. S. Babicki, *et al.*, Heatmapper: web-enabled heat mapping for all. *Nucleic Acids Res.* **44**, W147–W153 (2016).
66. N. C. Shaner, *et al.*, A bright monomeric green fluorescent protein derived from Branchiostoma lanceolatum. *Nat. Methods* **10**, 407–9 (2013).
67. J.-D. Pédelacq, S. Cabantous, T. Tran, T. C. Terwilliger, G. S. Waldo, Engineering and characterization of a superfolder green fluorescent protein. *Nat. Biotechnol.* **24**, 79–88 (2006).
68. B. S. Chambers, *et al.*, DNA mismatch repair is required for the host innate response and controls cellular fate after influenza virus infection. *Nat. Microbiol.* **4**, 1964–1977 (2019).
69. C. T. Workman, *et al.*, enoLOGOS: a versatile web tool for energy normalized sequence logos. *Nucleic Acids Res.* **33**, W389–W392 (2005).
70. G. Wei, *et al.*, Genome-wide analysis of ETS-family DNA-binding in vitro and in vivo. *EMBO J.* **29**, 2147–2160 (2010).

682 **Acknowledgements**

683 We would like to acknowledge Brook Heaton for generating the A549-CRISPR-SAM-
684 IFNrsp cell line. We acknowledge assistance from Mike Cook and the Duke Cancer
685 Institute Flow Cytometry Core. We thank Robert Lefkowitz and his laboratory for
686 assistance with and use of the ChemiDoc Imaging System. We also thank Ephraim Tsalik
687 and Micah McClain for helpful discussions and Ben Chambers, Stacy Webb, and other
688 members of the Heaton lab for critical reading of the manuscript. H.M.F. and A.T.H. were
689 supported by NIH training grant T32-CA009111. N.S.H. is supported by R01-HL142985,
690 R01-AI137031, and funding from the Defense Advanced Research Projects Agency's
691 (DARPA) PReemptive Expression of Protective Alleles and Response Elements
692 (PREPARE) program (Cooperative agreement #HR00111920008). The views, opinions
693 and/or findings expressed are those of the author and should not be interpreted as
694 representing the official views or policies of the U.S. Government.

695

696 **Author Contributions**

697 A.T.H. and N.S.H. designed the screen. A.T.H performed the screen experiments and
698 initial analysis. H.M.F. and N.S.H. designed the screen validation studies. H.M.F.
699 performed the screen hit determination analysis, flow cytometry, RNA and protein
700 quantification experiments, sequencing and promoter analysis, and virus infection
701 experiments. A.T.H. generated the Cal/09-sfGFP virus. H.M.F. and N.S.H. wrote the
702 manuscript.

703